

Comparison of expression patterns and cell adhesion properties of the mouse biliary glycoproteins Bgp1 and Bgp2

Julie Robitaille¹, Luisa Izzi^{1,2}, Eugene Daniels³, Bruce Zelus⁵, Kathryn V. Holmes⁵ and Nicole Beauchemin^{1,2,4}

¹McGill Cancer Centre and Departments of ²Biochemistry, ³Anatomy and Cell Biology, and ⁴Oncology and Medicine, McGill University, Montreal, Canada; ⁵Department of Microbiology, University of Colorado Health Sciences Centre, Denver, CO, USA

Biliary glycoproteins are members of the carcinoembryonic antigen (CEA) family and behave as cell adhesion molecules. The mouse genome contains two very similar *Bgp* genes, *Bgp1* and *Bgp2*, whereas the human and rat genomes contain only one *BGP* gene. A *Bgp2* isoform was previously identified as an alternative receptor for the mouse coronavirus mouse hepatitis virus. This isoform consists of two extracellular immunoglobulin domains, a transmembrane domain and a cytoplasmic tail of five amino acids. In this report, we have examined whether the *Bgp2* gene can express other isoforms in different mouse tissues. We found only one other isoform, which has a long cytoplasmic tail of 73 amino acids. The long cytodomain of the Bgp2 protein is highly similar to that of the Bgp1/4L isoform. The Bgp2 protein is expressed in low amounts in kidney and in a rectal carcinoma cell line. Antibodies specific to Bgp2 detected a 42-kDa protein, which is expressed at the cell surface of these samples. Bgp2 was found by immunocytochemistry in smooth muscle layers of the kidney, the uterus, in gut mononuclear cells and in the crypt epithelia of intestinal tissues. Transfection studies showed that, in contrast with Bgp1, the Bgp2 glycoprotein was not directly involved in intercellular adhesion. However, this protein is found in the proliferative compartment of the intestinal crypts and in cells involved in immune recognition. This suggests that the Bgp2 protein represents a distinctive member of the CEA family; its unusual expression patterns in mouse tissues and the unique functions it may be fulfilling may provide novel clues about the multiple functions mediated by a common BGP protein in humans and rats.

Keywords: biliary glycoprotein (BGP); carcinoembryonic antigen; C-CAM; CD66; cell adhesion.

Biliary glycoproteins (Bgps or BGPs, also known as C-CAM and CD66a) are members of the carcinoembryonic antigen (CEA) family within the immunoglobulin (Ig) family. The CEA gene family forms a large cluster of 29 genes which has been mapped to human chromosome 19q13.2 [1]. This gene family is divided according to the membrane anchorage of their gene products; the first subgroup of genes, which includes the *Bgp* gene, encode proteins that display cell surface attachment. Another subgroup within the same gene family, identified as the pregnancy-specific glycoprotein subgroup, encodes proteins secreted from the cells of the placenta. Whereas the human CEA gene family includes only one *BGP* gene, the mouse *Cea* gene family exhibits two highly similar *Bgp* genes, *Bgp1* and *Bgp2*, on the syntenic region of mouse chromosome 7 [2–4]. At least four different splice variants of the mouse *Bgp1* gene have been characterized (Fig. 1): these contain an N-terminal V-like Ig domain and express either one or three constant C2-set Ig-like domains [3]. Each Ig domain is encoded by a different exon. These Bgp1 splice variants also differ in the lengths of their cytoplasmic domains which may have either a 10-amino acid (short, S) or a 73-amino acid (long, L) tail [5]. The structure of the *Bgp1* and *Bgp2* genes and the splice

variants used in this study are highlighted in Fig. 1. Two allelic variants have been identified for the *Bgp1* gene in various mouse strains, *Bgp1^a* and *Bgp1^b* [6]. Our study was carried out using tissues from the BALB/c mouse, which expresses only the *Bgp1^a* allele, and, throughout this paper, the gene will be referred to as *Bgp1*. Bgp1/4L refers to the splice variant with four extracellular Ig-like domains and a long cytoplasmic domain, whereas Bgp1/2S and Bgp2/2S stand for the *Bgp1* and *Bgp2* gene products with two extracellular Ig-like domains and a short tail. sBgp2 represents the secreted Bgp2 protein.

Several functions have been described for Bgp1. The human, rat and mouse proteins function as homophilic intercellular adhesion molecules [7–9]. This function is instrumental in major tissue reorganization during embryonic development [10] such as hepatocyte aggregation [8]. We [11] and others [12] have also demonstrated that Bgp1 with the long cytoplasmic domain functions as a tumor-suppressor protein which inhibits the development of colonic and prostatic tumors in rodents. In addition, expression of human BGP is down-regulated in liver, breast and endometrial carcinomas [13–15]. The mouse Bgp1/4L protein is also involved in signal transduction. It can be phosphorylated on tyrosine residues by Src-like kinases and binds to the protein Tyr phosphatases SHP-1 and SHP-2 [16,17]. Tyr phosphorylation and activation of BGP leads to respiratory bursts in human neutrophils [18]. Binding of the *Neisseria gonorrhoeae* opa₅₂ membrane protein to human BGP expressed at the surface of neutrophils leads to enhanced Tyr phosphorylation of BGP and activation of Rac1, PAK and Jun-N-terminal kinases [19]. Murine Bgp1 and Bgp2 glycoproteins act as receptors for the murine coronavirus mouse hepatitis virus [20].

Correspondence to N. Beauchemin, McGill Cancer Centre, McGill University, McIntyre Medical Sciences Building, 3655 Drummond St., Montreal, Qué, Canada H3G 1Y6. Fax: + 514 398 6769, Tel.: + 514 398 3541, E-mail: nicoleb@med.mcgill.ca

Abbreviations: Bgp or BGP, biliary glycoprotein; CEA, carcinoembryonic antigen; Ig, immunoglobulin; SHP-1 and SHP-2, Src-homology phosphatases; CHO, chinese hamster ovary cells; RT-PCR, reverse transcription-PCR; GST, glutathione S-transferase.

(Received 5 May 1999; accepted 22 June 1999)

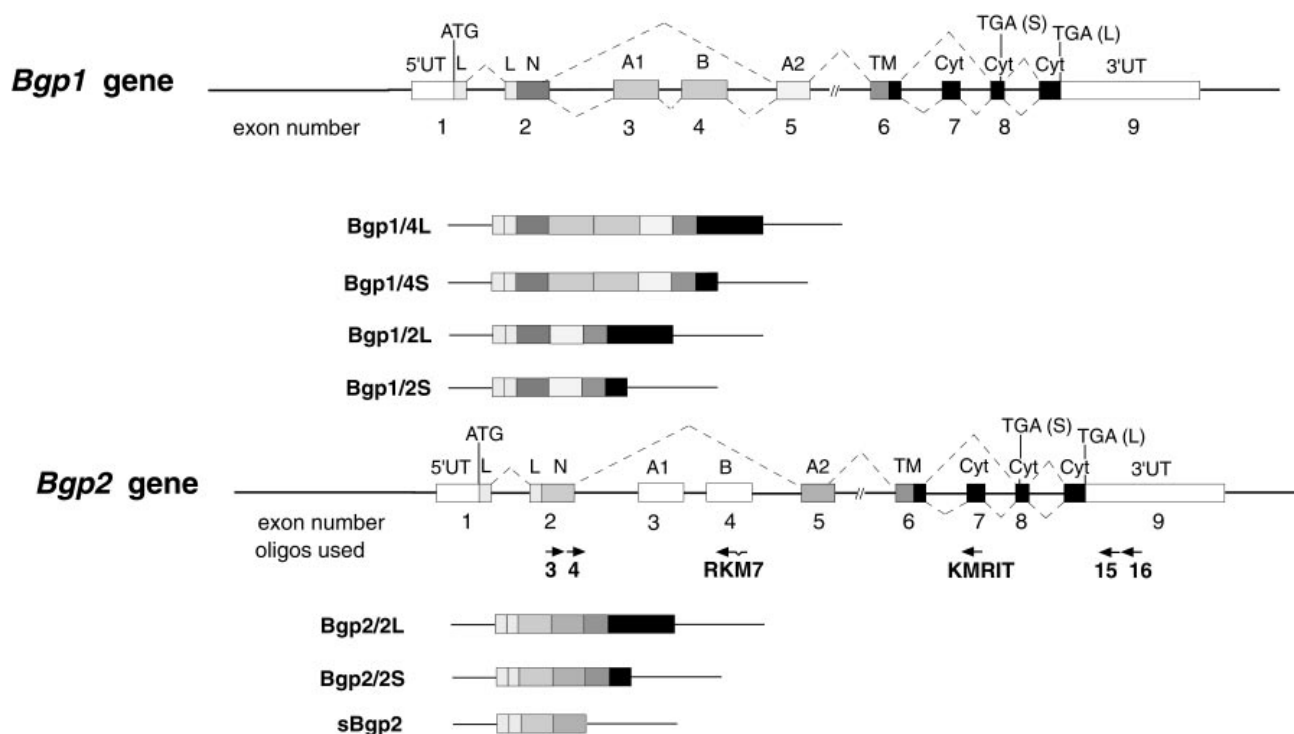


Fig. 1. Structure of the *Bgp1* and *Bgp2* genes and transcripts. The structure of the mouse *Bgp1* and *Bgp2* genes are highly similar in the intron/exon topology and in the length of the introns. Dashed lines represent the alternative splicing patterns giving rise to the respective *Bgp1* and *Bgp2* transcripts drawn under each gene. The translational start codon (ATG) as well as the stop codon specific for each transcript [TGA (S) or TGA (L)] are indicated. The 5' and 3' untranslated regions (5'UT and 3'UT) are included in the open boxes. L, Leader sequence; N, N-terminal domain; A1, B, A2 encode the C2-set Ig-like domains; TM, transmembrane domain; Cyt, the cytoplasmic domain. The arrows under the *Bgp2* gene or transcripts are the oligonucleotides used in the Southern-blot hybridizations in Fig. 2. The nomenclature for the *Bgp* transcripts is the following: the name of the gene (*Bgp1* or *Bgp2*)/the number of extracellular Ig-like domains followed by the length of the cytoplasmic tail. sBgp2, baculovirus-expressed His₆-tagged secreted Bgp2.

We identified and characterized the murine *Bgp2* gene and found that its genomic structure was remarkably similar to that of the *Bgp1* gene [3,4]. A specific *Bgp2* transcript was identified in the CMT-93 mouse rectal carcinoma cell line by RNase-protection analyses, and the corresponding cDNA was cloned and characterized [4]. Transient transfection of the *Bgp2* cDNA in hamster cells showed that the expressed protein was a functional receptor for mouse hepatitis viruses, albeit with less receptor activity than Bgp1 [4,21].

However, to date, only one splice variant of the *Bgp2* gene has been characterized. This transcript encodes two Ig-like exodomains, a transmembrane domain and a short cytoplasmic tail (*Bgp2/2S* in Fig. 1) [4]. Sequence differences were apparent between the murine *Bgp1* and *Bgp2* gene products; the predicted amino acid sequences diverge significantly in the first 37 residues of the mature proteins as well as within the central portion of the C2-set Ig-like domain. In addition, although the genomic structure predicted that a long cytoplasmic domain could be generated by the inclusion of the 53-bp exon 7, no such transcript was identified at that time. A number of questions about Bgp2 remain unanswered. The tumor-suppressive functions of Bgp1 in many types of cancer depend on the expression of its long cytodomain [11]. The *Bgp1* and *Bgp2* mRNAs were also found coexpressed in some tissues (such as small and large intestine). It therefore became essential to verify the expression pattern of the Bgp2 protein(s) in a larger screen and to identify whether a splice variant potentially expressing a long tail could indeed be detected in certain tissues.

Using reverse transcription-PCR (RT-PCR) amplifications, we have identified in murine kidney and CMT-93 cells a low

amount of *Bgp2* mRNA expressing a long cytoplasmic domain. The predicted sequence of the long cytodomain differs from Bgp1 by only four amino acids. However, no *Bgp2* transcripts encoding four Ig domains were found. Several polyclonal antibodies have been raised to purified murine Bgp2 fragments. Immunofluorescence staining using these antibodies demonstrated that the Bgp2 protein is localized at the surface of Chinese hamster ovary (CHO) cells transfected with the *Bgp2/2S* cDNA. Immunostaining of several mouse tissues showed that the Bgp2 protein is expressed in the smooth muscle layers of the kidney, gut and reproductive tissues. The Bgp2 protein is also found in the proliferative crypt region of the mouse intestine. The Bgp2 protein is expressed in mononuclear cells (macrophages) in the spleen and bone marrow. The cell adhesion activity of the Bgp2 protein stably transfected in CHO fibroblasts was examined. Unlike Bgp1, which is competent at intercellular adhesion, Bgp2 had no homophilic adhesion activity.

MATERIALS AND METHODS

RT-PCR amplifications and cloning of inserts

To detect novel transcripts of the *Bgp2* gene, amplification of first-strand cDNA, produced after the reverse transcription of total RNA from several adult BALB/c tissues or cell lines, was used. In brief, 25 µg of total RNA was subjected to reverse transcription using the avian myeloblastosis virus reverse transcriptase (Life Sciences, St Petersburg, FL, USA) at 42 °C for 2 h using oligonucleotide 16 (in the 3' untranslated region) within the previously published *Bgp2* cDNA sequence

in a total volume of 35 μL [4]. The resulting cDNAs were purified on Qiaquick columns (Qiagen), and 50% of the first-strand cDNAs was used to prime the synthesis of the second-strand cDNAs using oligonucleotides 3 (in the N-terminal domain) and 15 (in the 3' untranslated region) of the *Bgp2* cDNA sequence [4]. PCR amplifications were performed essentially as described previously by including the Vent DNA polymerase (New England Biolabs, Beverly, MA, USA) in the following program: denaturation at 94 °C for 40 s, annealing of primers 3 and 15 [4] at 53 °C for 2 min and extensions of 3 min at 72 °C for 35 cycles. The DNA fragments were separated by electrophoresis, transferred to Hybond N⁺ membranes (Amersham) and probed with [³²P]-labeled oligonucleotides specific for the *Bgp2* N-terminal domain (oligonucleotide 4), the long cytoplasmic domain of *Bgp1* (5'-TGAGGGTTTGTGCTCTGTGAGATC, oligonucleotide KMRIT) or the B exon of the *Bgp1* gene (5'-CCTCCAA-GAGCTCTTATC, oligonucleotide RKM7) according to procedures described previously [4]. The blots were washed in a solution of 0.1 \times NaCl/Cit containing 0.1% SDS at final stringencies of 37 °C for oligonucleotide 4, 50 °C for the oligonucleotide KMRIT within the cytoplasmic domain, and 20 °C for the oligonucleotide RKM7 within the third Ig domain. Possible cross-hybridization between *Bgp1* and *Bgp2* cDNAs was monitored by including the appropriate controls on the Southern blots, such as the *Bgp1/4L* cDNA and the *Bgp2/2S* cDNA which contained a shorter 3' untranslated region than the RT-PCR-amplified cDNAs. The fragments identified in these analyses were separated on 1% agarose gels and the extracted cDNA cloned into pPCRScript (Stratagene). The cDNA was sequenced using the dideoxy chain-termination technique [22].

Tissues and cells used

Fresh tissues were excised from adult BALB/c mice. The mouse WEHI 231 B-lymphocytic cell line, the RAW264 macrophage cell line and a bovine insulin-specific mouse hybridoma T-cell line (BI-141) were kindly provided by André Veillette (McGill University, Montreal, Canada). These cells were grown in either RPMI 1640 or minimal essential medium (α -MEM) supplemented with 10% heat-inactivated fetal bovine serum (Gibco), 2 mM glutamine, 50 U·mL⁻¹ penicillin and 50 $\mu\text{g}\cdot\text{mL}^{-1}$ streptomycin. The CMT-93 mouse rectal carcinoma cell line was purchased from the American Type Culture Collection and grown as indicated above. LR73 CHO transfectant cells expressing the *Bgp1* protein with either the long or short cytoplasmic tails have previously been described [9,23]. *Bgp2/2S*-expressing LR73 CHO fibroblasts (1 \times 10⁵ cells·100 mm dish⁻¹) were generated by cotransfection of 5 μg of the p91023B vector containing the *Bgp2/2S* cDNA and 0.5 μg of the pSV2neo plasmid using the calcium phosphate coprecipitation technique [24]. The p91023B vector uses the major late adenoviral promoter to drive the transcription of the inserts. Similarly, a *Bgp1/2S* cDNA (Fig. 1) cloned into the p91023B vector was also transfected into LR73 CHO cells under identical conditions. Transfected cells were selected with G418 (1 mg·mL⁻¹) for 10 days, and cell clones were manually isolated from the cell populations. Evaluation of the *Bgp2/2S* mRNA expression was determined by Northern-blot analyses on 20 μg of total cellular RNA isolated from the transfectant cell clones according to standard procedures [25], using the *Bgp2/2S* cDNA as a probe. Expression of the *Bgp2/2S* protein was detected by immunoblotting 100 μg of total cellular proteins using the anti-*Bgp2*-specific rabbit antibody 2052. A transfected NIH 3T3 cell clone expressing the *Bgp1* cDNA

with four Ig domains (*Bgp1/4S*) has previously been described [9].

Antibodies

First, a multiple-antigen-peptide-coupled peptide [26], encompassing amino acids 57–74, which are unique to the *Bgp2* protein, was synthesized at the Montreal Biotechnology Research Institute. A 10–50 μg portion of this peptide was used to raise antibodies in rabbits (Ab 980). Second, glutathione S-transferase (GST) fusion proteins consisting of either of the two Ig domains of the *Bgp2* protein, corresponding to amino acids 35–142 and 142–232, were prepared. Two PCR fragments were amplified from the *Bgp2/2S* cDNA template using the following oligonucleotides: in the N-terminal domain, the forward oligonucleotide was 5'-CAAGTGACTGTTATGGC and the reverse oligonucleotide was 5'-TTGTGTACATGAAA, while in the C2-set Ig domain the forward oligonucleotide was 5'-CAAGCCAGTGACTCAG and the reverse oligonucleotide was 5'-TATTACTTCCAGTTT. Each of these fragments was cloned into the *Sma*I site of the pGEX2T vector, and the plasmids were transformed into BL21 *Escherichia coli* bacteria. Fusion proteins were induced for 6 h using 0.1 mM isopropyl thiogalactoside and purified by adsorption on glutathione-Sepharose beads according to published procedures [27]. Antibodies were then raised in rabbits to these purified proteins (Ab 1818 to the N-terminal domain, Ab 1687 to the second Ig-like domain). A rabbit antibody, 2052, was also raised to the purified secreted *Bgp2* protein (s*Bgp2*) expressed in a baculovirus vector. A *Bgp2* cDNA fragment including nucleotides 1–829, corresponding to amino acids 1–243 in the extracellular domains of the *Bgp2* protein, was cloned into pAcMP2 (PharMingen, San Diego, CA, USA). Sequences encoding a thrombin-cleavage site and a hexahistidine tag were added on to the C-terminus of s*Bgp2* [21]. The baculovirus-expressed His₆-tagged soluble *Bgp2* protein was purified using HisTrap Ni-chelating and Mono Q columns (Pharmacia) [21], and the purified material was used to raise polyclonal antiserum 2052 in rabbits. An IgG fraction of this antiserum was prepared by adsorption on a Protein A-Sepharose column. The rabbit polyclonal antibodies raised to the long cytoplasmic domain of the *Bgp1* protein (Ab 836) and to the *Bgp1* protein (Ab 231) have previously been described [9,23].

Immunoprecipitation and immunoblotting

Cells were detached from the culture dishes by scraping or using a solution of NaCl/P_i/citrate and processed for protein lysates. Fresh BALB/c mouse tissues were frozen on dry ice, powdered using a cold mortar and pestle, and the resulting cell paste was lysed on ice for 10 min in buffer containing 50 mM Tris/HCl, pH 8.0, 10 mM EDTA, 1% Nonidet P40 and 10 $\mu\text{g}\cdot\text{mL}^{-1}$ each of the following protease inhibitors: leupeptin, pepstatin, aprotinin, phenylmethanesulfonyl fluoride, Tos-Lys-CH₂Cl and Tos-Phe-CH₂Cl. Soluble proteins were recovered after a 10-min centrifugation at 4 °C at 15 000 g. Total protein concentration was determined using a BCA Protein Assay kit (Pierce Chemicals, Rockford, IL, USA). Cell lysate proteins (100–200 μg) were resolved by SDS/PAGE (10% gels), the proteins were transferred to Immobilon membranes and Bgps were detected by incubation with the polyclonal Ab 231 (anti-*Bgp1*) [8] or Ab 2052 (anti-*Bgp2*) and [¹²⁵I]-labeled Protein A (ICN).

Immunoprecipitation analysis on cell or tissue proteins was performed by incubation of 250–1000 μg of total cellular

proteins with Ab 231 (anti-Bgp1), Ab 836 (specific to the long Bgp1 cytoplasmic domain) or Ab 1687 or 2052 (anti-Bgp2) for 2–18 h at 4 °C. The immune complexes were collected on Protein A–Sepharose beads, separated by SDS/PAGE (10% gels), and the resolved proteins detected by immunoblotting as described above.

Immunofluorescence and immunocytochemistry

Cells stably transfected with the Bgp1/2S or Bgp2/2S cDNAs were grown on coverslips, fixed with Bouin's fixative, then permeabilized with 0.5% Nonidet P40 in 1% BSA/heat inactivated normal goat serum/NaCl/P_i. The cells were incubated for 1 h with either anti-Bgp1 (Ab 231) or anti-Bgp2 (Ab 2052) antibodies. After extensive washes, the complexes were treated for 30 min with 4.4 µg·mL⁻¹ Cy3-labeled goat anti-(rabbit IgG) (Jackson). The cells were visualized and photographed on a Nikon fluorescence microscope.

Immunohistochemical staining of fixed paraffin-embedded sections of adult BALB/c tissues was performed using the peroxidase–antiperoxidase procedure [10]. Endogenous peroxidase activity in the deparaffinized sections was blocked with methanol/peroxide solution. Incubation with the primary antibodies (Abs 231, 980, 1687 and 2052) was carried out in a wet chamber overnight at 4 °C. After washes in Tris buffer and incubations with secondary antibodies [swine anti-(rabbit IgG), 1 : 50], subsequent rabbit peroxidase–anti-peroxidase immunostaining (1 : 250) was revealed by controlled 3'-diaminobenzidine tetrahydrochloride reactions [10]. Bone marrow suspension cells were prepared for immunocytochemical studies using a Shandon Cytospin 2 centrifuge. Sections were lightly stained with hematoxylin and photographed with a digital photomicroscope.

Adhesion assays

Cell-aggregation assays were performed using either wild-type LR73 CHO cells or cell clones stably transfected with either the Bgp1/2S or Bgp2/2S cDNA constructs or an empty control vector. Cells were removed from the tissue culture dishes with a solution of NaCl/P_i/citrate containing 0.125% trypsin, and made into single cell suspensions by three passages through 27-gauge needles. Viability of cells determined by trypan blue dye exclusion was shown to be > 95% in every assay. A total of 3 × 10⁶ cells of each transfectant clone was incubated in 3 mL of α-MEM containing 0.8% fetal bovine serum and DNase I (Boehringer Mannheim; 10 µg·mL⁻¹) for 2 h at 37 °C with constant stirring at 100 r.p.m.; samples were retrieved at regular intervals to evaluate with a hemocytometer both single cells and number of cells per aggregate [9]. Adhesion assays were repeated three times with each cell line. Three measurements were taken at each time point and the mean of nine results used to plot the figure. Standard deviations and standard errors were obtained according to Student's *t* test.

RESULTS

Identification of Bgp2 transcripts

As seen in Fig. 1, the murine *Bgp1* and *Bgp2* genes are very similar in their structural features [3,4]. *Bgp1* alternatively spliced transcripts have been identified that include either two or four extracellular Ig domains and either a short or long

cytoplasmic domain (Fig. 1) [3,5]. In contrast, in our initial studies on clones from the CMT-93 mouse rectal carcinoma cell line, only one *Bgp2* transcript was detected, that encoding a Bgp2 protein with an N-terminal and a C2-set Ig-like domain and a short cytoplasmic tail (Bgp2/2S, Fig. 1) [4]. To verify whether other *Bgp2* transcripts might become apparent in different tissues, we used an RT-PCR amplification approach, as described in Materials and methods. *Bgp2*-specific oligonucleotides were used to amplify cDNAs from adult BALB/c mouse colon, kidney, non-pregnant uterus and liver and from the CMT-93 rectal carcinoma cell line. These samples had previously been shown to express the Bgp2 N-terminal domain by RNase-protection analyses [4]. To detect cDNAs of novel *Bgp2* transcripts, we hybridized representative Southern blots first with an oligonucleotide specific for the Bgp2 N-terminal domain (oligonucleotide 4, Figs 1 and 2A), then with an oligonucleotide specific for the *Bgp1* and *Bgp2* cDNA encoding the long cytoplasmic domain (KMRT, Figs 1 and 2B), and finally to an oligonucleotide corresponding to the third Ig domain of the *Bgp1* gene (RKM7, Figs 1 and 2C). The last two oligonucleotides were designed according to the DNA sequence of the *Bgp1* and *Bgp2* exons ([4]; P. Nédellec and N. Beauchemin, unpublished data). As can be seen in Fig. 2A, a single *Bgp2* cDNA of 1050 bp was detected in the kidney and CMT-93 samples with the oligonucleotide specific to the *Bgp2* N-terminal domain. The cDNA sequence of this fragment corresponded to the *Bgp2/2S* cDNA already identified [4]. No other transcripts were detected by Southern blotting, even at low wash stringencies. However, another *Bgp2* cDNA with a long cytoplasmic domain differed only by the inclusion of the 53-bp exon 7 (Fig. 3) [4], and migrated very close to the cDNA shown in Fig. 2A. Therefore, we used an oligonucleotide corresponding to the *Bgp2* exon 7 sequence; this oligonucleotide binds equally well to a *Bgp1* cDNA including the long cytoplasmic domain (Bgp1/4L), as their *Bgp1* and *Bgp2* genomic sequences are identical in this region. When hybridized to the amplified *Bgp2* cDNAs, the same cDNAs as seen in Fig. 2A were indeed positive for this oligonucleotide (Fig. 2B, lanes 3 and 5), as was the *Bgp1/4L* cDNA (Fig. 1B, lane 1). However, neither the *Bgp1/2S* nor *Bgp2/2S* cDNAs containing the short cytoplasmic domains hybridized with this oligonucleotide (Fig. 1B, lanes 8 and 9), demonstrating the specificity of the hybridization procedure. When the same Southern blot was washed and rehybridized with an oligonucleotide specific for the third Ig domain of the *Bgp1/4L* cDNA, which has one nucleotide difference from *Bgp2* exon 4, no *Bgp2* cDNAs were detected (Fig. 2C, lanes 2–7). These results indicate that *Bgp2* mRNAs that include the N-terminal and fourth Ig-like domains and either the short or the long cytoplasmic domain were transcribed in the kidney and in the CMT-93 cell line; however, the *Bgp2/2L* transcript was expressed very weakly in colon (visible after two rounds of PCR amplifications) and not at all in mouse non-pregnant uterus and liver.

Characterization of the Bgp2 long cytoplasmic domain

We and others have demonstrated that Bgp1/4L participates in important cellular functions. This Bgp1 isoform has tumor-suppressor functions and participates in signal-transduction events as described in the Introduction. It therefore became important to characterize the Bgp2 cytoplasmic domains more fully. The cDNA fragments of *Bgp2/2L* were cloned and sequenced. The cDNA sequence of the *Bgp2/2L* variant has been deposited in GenBank under the accession number

AF101164; the corresponding protein translation of the cytoplasmic domains is presented in Fig. 3. As previously demonstrated [3,4], the *Bgp1* and *Bgp2* splice variants bearing the short cytoplasmic domain are produced from the joining of

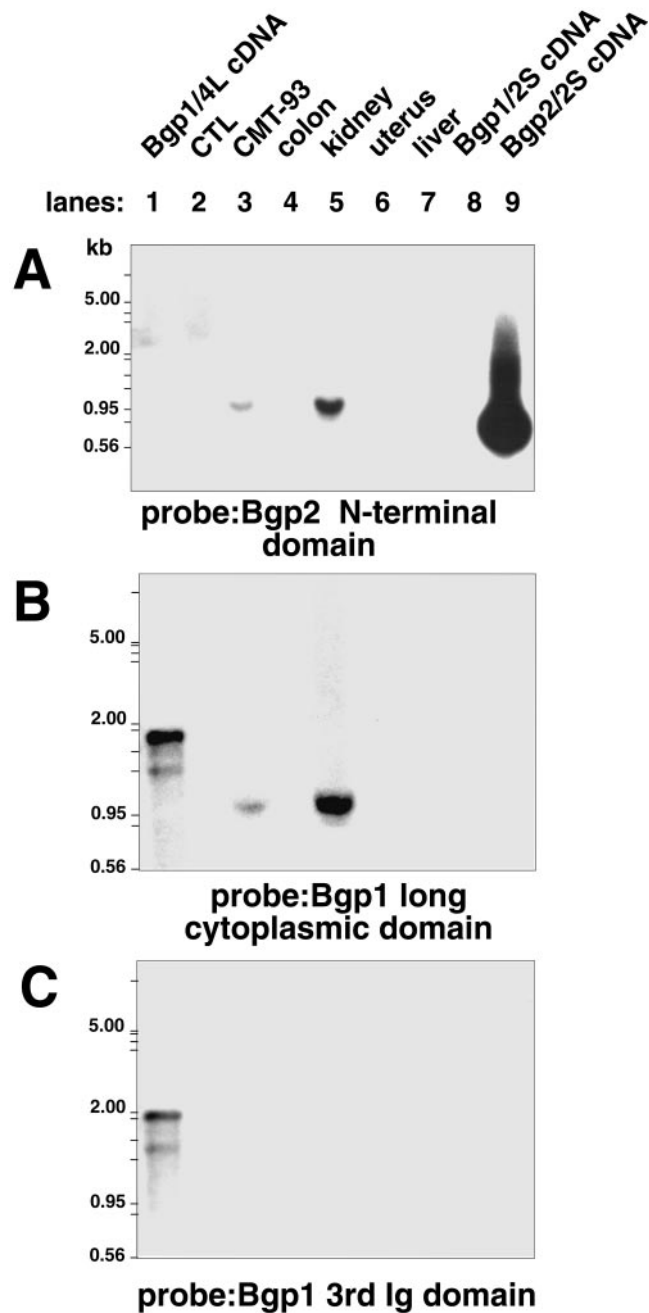


Fig. 2. Southern-blot analyses of the RT-PCR products. RT-PCR amplifications of total RNA prepared from different tissues or cell lines were performed as described in Materials and methods, and the products separated on 1% agarose gels and transferred to membranes. The presence of novel *Bgp2* cDNAs was revealed by hybridization of the membranes with [³²P]-labeled oligonucleotides indicated in Fig. 1, specific to the N-terminal domain of the *Bgp2* cDNA (oligonucleotide 4) (A), the *Bgp1/L* cytoplasmic region (oligonucleotide KMRIT) (B) or the third Ig domain (oligonucleotide RKM7) of the *Bgp1* protein (C). CTL, control with no DNA. The RNA used in these experiments was extracted from adult BALB/c mouse tissues. As controls of hybridizations, the previously cloned *Bgp1/4L*, *Bgp1/2S* and *Bgp2/2S* cDNAs were included.

exons 6 and 8 of their respective genes (Fig. 3A). This results in the presence of an in-frame stop codon (TGA) immediately at the junction of these two exons of the *Bgp2* gene, yielding a cytoplasmic domain shorter by five amino acids than the *Bgp1/2* or *4S* splice variants (Fig. 3A). As predicted by the genomic structure, however, the *Bgp2* long tail is assembled by the inclusion of the 53-bp fragment including exon 7 which becomes inserted between nucleotides 916 and 917 of the published *Bgp2/2S* cDNA sequence [4]. The insertion of this exon converted a TG↓A stop codon used in the short cytoplasmic form to a TG↓G Trp codon (Fig. 3B). The 53-bp added fragment was followed by a nucleotide sequence which, in the short-tail-containing *Bgp2/2S* cDNA, corresponded to the 3' untranslated region, but which in the long tail variant became the coding region because of the number of nucleotides in exon 7 and the absence of an in-frame stop codon. The *Bgp2* long cytoplasmic domain is very similar to that of *Bgp1* apart from the divergence previously observed [4] in the proximal membrane region. When the human, rat and mouse *Bgp1* and *Bgp2* long tails were aligned (Fig. 3B), a number of conserved features were highlighted: for example, an SRKS/T motif (underlined in Fig. 3B) is present in the membrane-proximal area of the rat and mouse *Bgp* proteins, but is absent from the human *BGP* sequence. The Ser/Thr residues in this motif in the rat C-CAM have been shown to be phosphorylated in response to phorbol ester-induced activation of protein kinase C [28]. Although the SRKS sequence is well conserved between the *Bgp1* and *Bgp2* cytoplasmic tails, it is noticeable that, immediately flanking these residues, lie charged or bulky residues which may affect the conformation of the proteins in the membrane-proximal area. Another conserved feature is represented in the protein sequences encoded by exon 7 (large dark arrowheads in Fig. 3B), which are well conserved between the *BGP* genes in every species. Finally, the *Bgp2* long tail also has peptide sequences surrounding the two conserved Tyr residues like those of *Bgp1* (Fig. 3B, shaded) and these are phosphorylated by various cellular protein kinases [16,17].

Specificity of the anti-*Bgp2* antibodies

To verify whether the *Bgp2* transcripts detected led to the translation of a *Bgp2* glycoprotein, specific anti-*Bgp2* antibodies were raised. We took advantage of the significant sequence differences within the N-terminal domains and the Ig C2-set domain of the *Bgp1* and *Bgp2* proteins in designing either short peptides or longer ones fused with the GST fusion partner protein to raise polyclonal rabbit antibodies to *Bgp2*. Although all three antibodies raised recognized either their respective immunogens or the *Bgp2* in its native conformation as presented in tissue sections, they reacted only poorly with denatured *Bgp2* upon immunoblotting (data not shown). Ab 2052 was raised against a purified *Bgp2* protein produced in a baculovirus overexpression system [21]. To define the specificities of the anti-*Bgp1* and anti-*Bgp2* antibodies, immunoprecipitation and immunoblotting experiments were performed. The apparent molecular mass of the s*Bgp2* protein produced by the baculovirus was 31–33 kDa, consistent with glycosylation within the baculovirus system (Fig. 4A, lane 2). A single band was detected on the immunoblots with Ab 2052. The 2052 anti-*Bgp2* antibody immunoprecipitated the His₆-tagged *Bgp2* protein as seen in Fig. 4B, lane 2, but did not detect immune complexes of the *Bgp1* protein under similar conditions (Fig. 4B, lane 1), nor did it recognize the *Bgp1* protein in immunoblotting experiments (Fig. 4A, lane 1). Conversely, the anti-*Bgp1* 231 Ab was highly specific for the *Bgp1* protein in

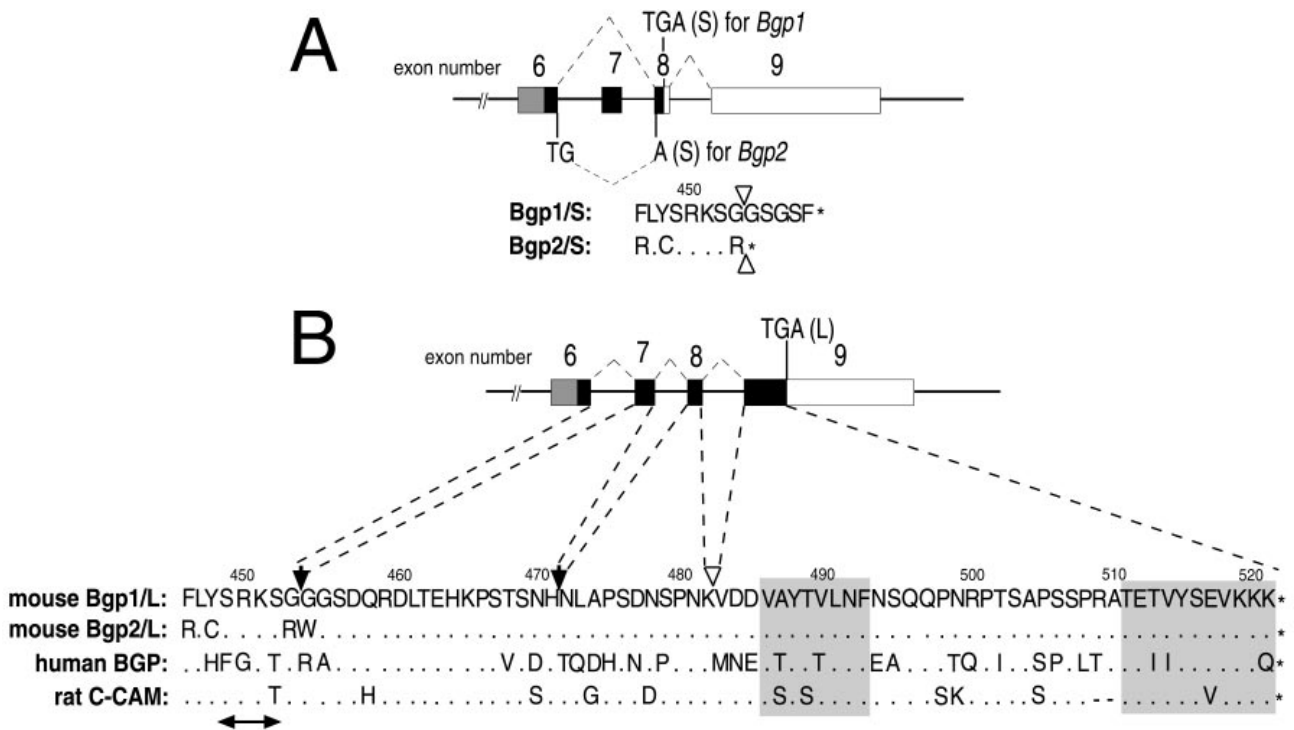


Fig. 3. Sequence alignments of the Bgp1 and Bgp2 cytoplasmic domains. The genomic organization and amino acid sequence of the Bgp2 cytoplasmic domains are shown. The positions of the stop codons for the *Bgp1* and *Bgp2* genes are indicated. The open triangles above or below the amino acid sequence represent the borders of the exons. The dark arrowheads delimit the amino acids encoded by exon 7. The underlined sequence in (B) corresponds to the protein kinase C phosphorylation site. The shaded areas define the conserved sequences around the Tyr-phosphorylated residues.

both immunoblotting and immunoprecipitation experiments (Fig. 4A,B, lanes 3 and 4). The protein band detected at ≈ 55 kDa in Fig. 4B, lanes 3 and 4, corresponds to a band detected by the preimmune 231 serum [23]. Therefore, the anti-Bgp2 2052 antibody raised with the baculovirus-produced sBgp2 protein is specific for the full-length, native and denatured Bgp2 protein.

Expression of the Bgp2 protein in adult mouse tissues

In our initial analyses of the *Bgp2* transcript(s) by RNase-protection assays, a fragment corresponding to the *Bgp2* mRNA was detected in BALB/c kidney, in CD1 spleen and CMT-93, a rectal carcinoma cell line [4]. The *Bgp2* transcript was barely detectable in the colonic tissue. To investigate whether a Bgp2 protein was translated from this transcript, combinations of immunoprecipitations and immunoblotting were performed with anti-Bgp2 antibodies. Positive controls to monitor the expression of the Bgp2 protein in tissues were produced by transfection of LR73 CHO cells with the *Bgp2/2S* cDNA. As can be seen in Fig. 5A, the parental LR73 CHO cells did not express any detectable Bgp2/2S protein (lane 5), while Bgp2/2S-transfected clones 80 and 1 expressed high and low amounts of the Bgp2/2S protein, respectively (Fig. 5A, lanes 3 and 4). In this case, the expressed protein migrated as a smear of ≈ 40 – 42 kDa, which corresponds to the predicted molecular mass of the mature protein given that Bgp2/2S has four potential N-linked glycosylation sites. The kidney was found to express protein bands migrating as a smear corresponding to those observed in the transfected clones (Fig. 5A, lane 7). In addition, in kidney, another protein band migrating as a 50–55-kDa band was observed. The identity of this protein is unknown. A single protein band was noticed in the CMT-93

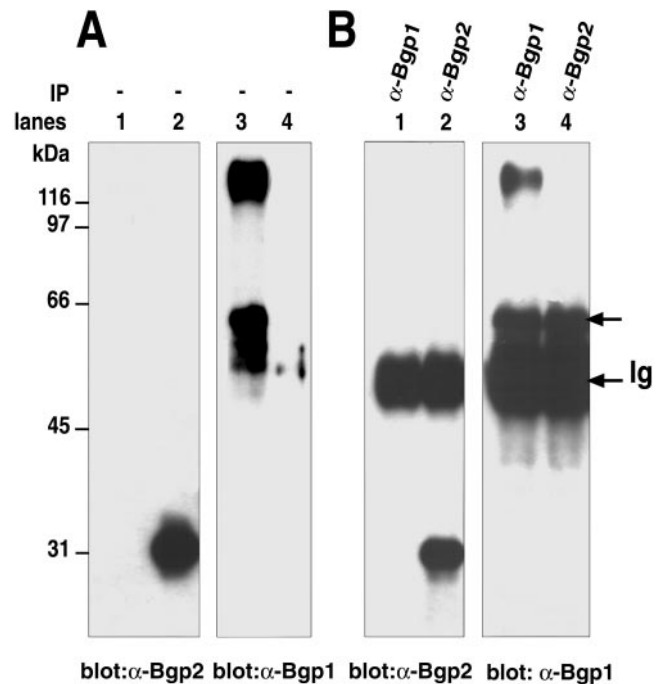


Fig. 4. Specificity of the anti-Bgp antibodies. (A) Immunoblotting and (B) immunoprecipitation of Bgp1 and Bgp2 proteins. Bgp1/4L-transfected NIH 3T3 total cell lysate proteins (100 μ g; lanes 1 and 3) and purified sBgp2 protein (10 μ g; lanes 2 and 4) were separated by SDS/PAGE (10% gels) after being subjected (B) or not (A) to immunoprecipitation with an anti-Bgp1 (Ab 231) or anti-Bgp2 (Ab 2052) antibody. The Bgp proteins were detected with the antibodies indicated below the blots. The positions of the molecular-mass markers are indicated on the left and the position of the Ig heavy chain on the right. The unlabeled arrow on the right represents an unspecific band also observed in the preimmune serum.

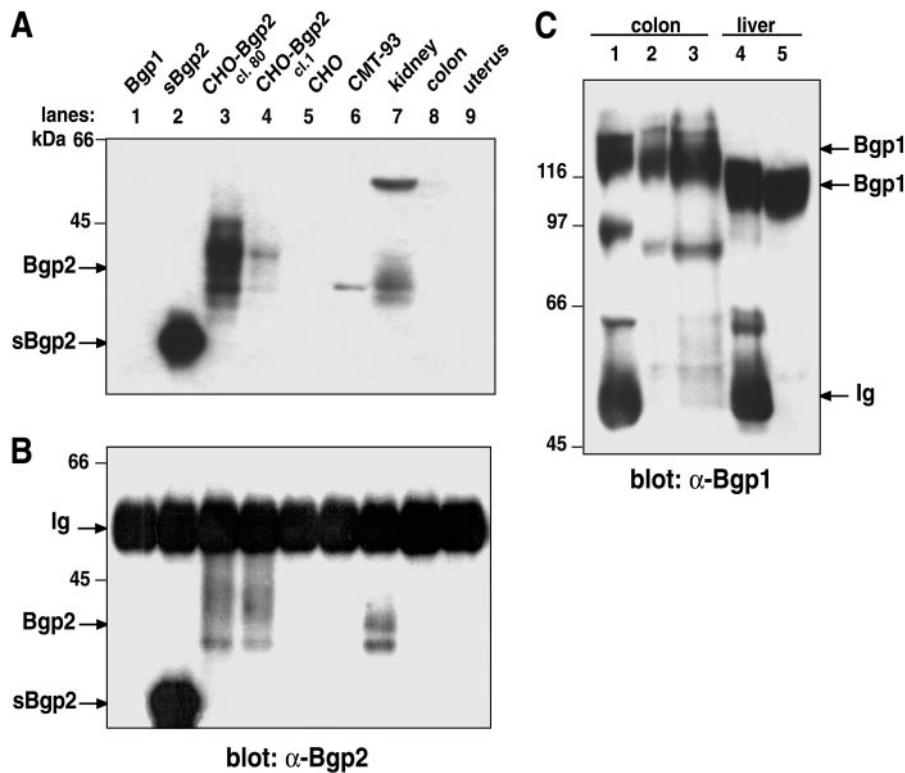


Fig. 5. Expression of Bgps in different tissues. (A) Immunoblotting and (B) immunoprecipitation of Bgp2 from different mouse tissues and cell lines. Total cell lysate proteins from Bgp1-transfected and Bgp2-transfected cells (100 μ g; lanes 1, 3–5), purified sBgp2 protein (10 μ g; lane 2) and total proteins (200 μ g; lanes 6–9) were separated by SDS/PAGE (10% gels) after being subjected (B) or not (A) to immunoprecipitation with anti-Bgp2 (Ab 1687) antibody. The blots were revealed with anti-Bgp2 antibody (Ab 2052). (C) Total proteins (200 μ g) from mouse colon and liver were immunoprecipitated (lanes 1 and 4) or not (lanes 2, 3, 5) with an anti-Bgp1 antibody (Ab 231). The proteins were revealed with the anti-Bgp1 antibody. The positions of the Bgp2, Bgp1 and Ig heavy chain proteins are indicated on the left or right of the membranes.

rectal carcinoma cells with an approximate molecular mass of 40 kDa (Fig. 5A, lane 6). When the Bgp2 protein was apparently more abundant [such as in kidney or the CHO-Bgp2-transfected clone 80 cells (Fig. 5A, lanes 3 and 7)], the major Bgp2 protein band was found within a smear corresponding to a number of glycoforms. No Bgp2 protein was detected in colon, uterus (Fig. 5A, lanes 8 and 9), liver and spleen samples (data not shown), nor was the Bgp2 protein detected in the B, T or macrophage cell lines described in Materials and methods.

When these samples were immunoprecipitated with the anti-Bgp 22052 antibody, similar results were obtained (Fig. 5B); however, the CMT-93-expressed Bgp2 protein was undetectable in these conditions (Fig. 5B, lane 6). These results suggest that the proteins revealed at 40–42 kDa do indeed correspond to Bgp2. For comparison, the same amounts of protein lysates from colon and liver were immunoprecipitated and immunoblotted with anti-Bgp1 Ab 231 under the same experimental conditions. As seen in Fig. 5C, intense bands of 105–110 kDa in liver (Fig. 5C, lanes 4 and 5) and 120 kDa in colon (Fig. 5C, lanes 1–3) were detected with this antibody. Other fainter signals apparent in the colon samples correspond to cleavage products of Bgp1, as discussed elsewhere [23]. The long cytoplasmic domains of the Bgp1 and Bgp2 proteins are nearly identical (Fig. 3B) and we therefore attempted to immunoprecipitate the Bgp2/2L isoform from either kidney or CMT-93 lysates with Ab 836, specific for the Bgp1 longer cytoplasmic domain. However, no Bgp2/2L protein isoform was detected in either samples upon immunoblotting with the anti-Bgp2 antibody (data not shown). Thus, the kidney and a mouse rectal carcinoma cell line both exhibited detectable levels of the Bgp2/2S protein whereas little or no Bgp2 protein could be detected in colon or uterus by this method. These results also suggest that Bgp2 may only be expressed at very low levels in colon, as observed previously in RNase-protection assays [4] and in RT-PCR amplifications.

To determine whether the Bgp2 protein was translocated appropriately and anchored to the cell surface, CHO cells expressing the mouse Bgp1/2S or Bgp2/2S proteins were labeled with specific antibodies and the proteins detected by immunofluorescence. Cells expressing the Bgp1/2S isoform displayed the protein at the surface of the cells, and the Bgp2 glycoprotein was also expressed at the cell surface (data not shown). The same transfected cells were negative with the secondary antibody alone. Wild-type or control transfected cells were also negative with the primary and secondary antibodies (data not shown).

Immunocytochemistry

In order to detect which cell types in various mouse tissues expressed the Bgp2 proteins, immunohistochemical staining was performed with several anti-Bgp2 antibodies. The reactions observed with the anti-Bgp2 polyclonal antibodies 980, 1818 and 1687 were all identical with those observed with antibody (2052) raised to the baculovirus-expressed sBgp2 protein. It is also apparent that these antibodies recognize the Bgp2 protein more efficiently in tissue sections than under immunoprecipitation or immunoblotting conditions (see previous section). One noticeable feature of the Bgp2 protein was its expression in the cytoplasm of blood vessel smooth muscle cells in all organs, in the muscularis mucosa of the gut (Fig. 6A), in the lung (data not shown), in the uterus (Fig. 6C) and in calyces of the kidney (Fig. 6D). The immunostaining with the anti-Bgp2 antibodies was specific, as adjacent sections treated with the preimmune serum did not show any reactivity (Fig. 6C,D, top panel). In addition, migratory mononuclear cells (macrophages) were strongly labeled in the gut with the anti-Bgp2 antibodies (Ab 2052 and 980) (Fig. 6B), whereas leucocytes were more strongly labeled with the anti-Bgp1 antibody (231; Fig. 6G and [29]). Tissues in which both Bgp1 and Bgp2 were coexpressed did show significant differences in distribution

and intensity. In the small and large intestine, Bgp1 was identified in the crypt and villus epithelia [10], whereas Bgp2 was restricted to the crypt epithelia in the small intestine (Fig. 6A). Bgp2 also was detected on mononuclear cells in the

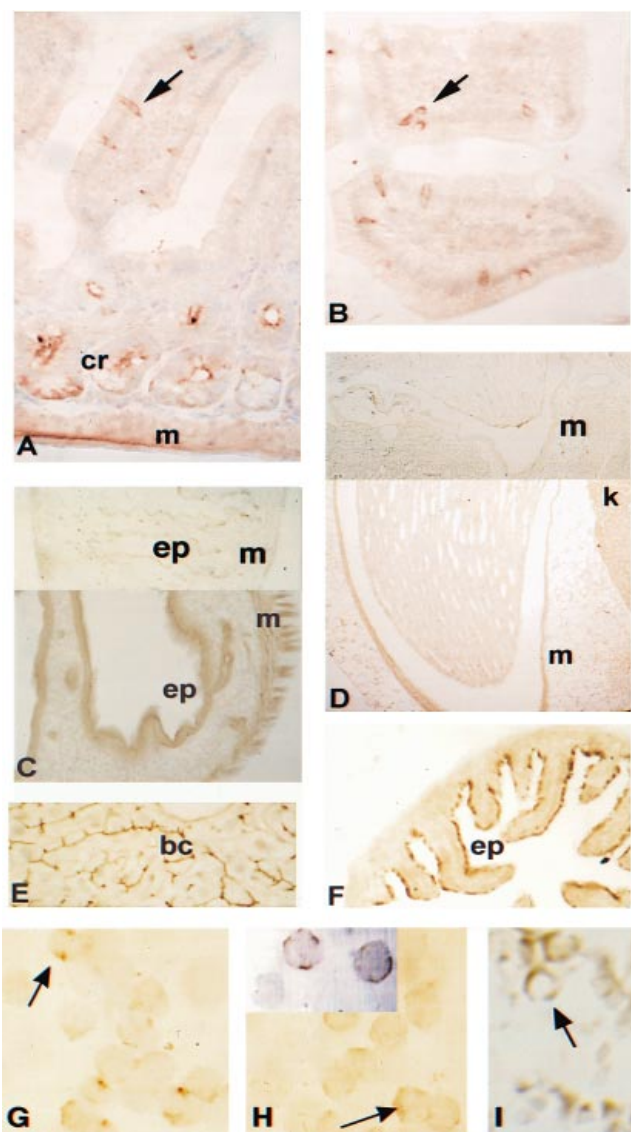


Fig. 6. Immunocytochemistry. Immunocytochemical reactions on adult BALB/c mouse tissues are indicated by the dark staining precipitates. (A) Positive reactions (anti-Bgp2 antibody; Ab 2052) are seen in the small intestine smooth muscle (m) crypts (cr) as well as in mononuclear cells in the lamina propria (arrow). (B) A higher magnification of the groups of mononuclear cells seen in lamina propria (arrow) and epithelium is shown. (C, bottom) Bgp2 expression was detected with Ab 2052 in the uterine epithelium and glands (ep) and smooth muscle (m) as well as in the oviduct shown (F). (C, top) Adjacent sections of the uterus were subjected to staining with the preimmune serum rabbit Ab 2052. (D, bottom) In the kidney, a strong reaction with anti-Bgp1 antibodies was identified in the smooth muscle seen in the minor calyces (m) as well as a diffuse reaction in the kidney epithelial cells (k). (D, top) This reaction was absent with the preimmune serum. (E) Staining of bile canaliculi with anti-Bgp1 antibodies shows a strong reaction. (F) Oviduct epithelium (ep) is positive with anti-Bgp2 antibodies. (G) Bone marrow cytospot shows positive reaction for Bgp1 in granulocytes (arrow). (H) A positive reaction to anti-Bgp2 antibodies (2052) is seen in bone marrow mononuclear cells (arrow, also inset), and in the spleen *in vivo* (I).

villi and crypts (Fig. 6A,B). Under light microscopy, no Bgp2 was detectable in the liver (data not shown), whereas Bgp1 was heavily concentrated in the bile canaliculi (Fig. 6E and [29]). In addition, no endothelial cell labeling was seen with Bgp2. The high concentration of Bgp2 in adult kidney seen on immunoblotting and RT-PCR analyses can be accounted for by the diffuse expression seen in cortical kidney epithelial cells (Fig. 6D), together with expression in the smooth muscle of the calyces (Fig. 6D) and blood vessels (data not shown). Bgp2 labeling in the reproductive system was found in the smooth muscle, uterine and endometrial epithelia and glands (Fig. 6C), although no specific expression had been detected in Southern blotting (Fig. 2) or immunoblotting (Fig. 5) experiments. In addition, the epithelial cells of the oviducts stained strongly with Bgp2 (Fig. 6F). Large mononuclear cells, suggestive of macrophages, were found to stain for Bgp2 in the bone marrow cytospot preparations (Fig. 6H) and in histological sections of adult spleen (Fig. 6I).

Bgp2 does not function as a cell adhesion molecule

The BGP proteins identified in human, mouse and rat have all been shown to function *in vitro* as homophilic intercellular adhesion molecules [7–9]. In each case, the first Ig domain was essential for the adhesion functions [30–32]. As the Bgp1 and Bgp2 proteins displayed significant differences in the primary amino acid sequences within the first Ig domain, we tested the ability of the Bgp2 protein to form cellular aggregates in a homophilic manner. Bgp1/2S- or Bgp2/2S-expressing CHO transfectant cells were suspended as single cells, and the development of cell clumps was monitored over a 2-h time period. As previously observed with the Bgp1/4S isoform [9], the Bgp1/2S isoform also induced intercellular adhesion, with 50% of the cells forming cellular aggregates during a 2-h time course (Fig. 7). When tested under similar conditions, the Bgp2/2S-transfected CHO cells remained as single cells and

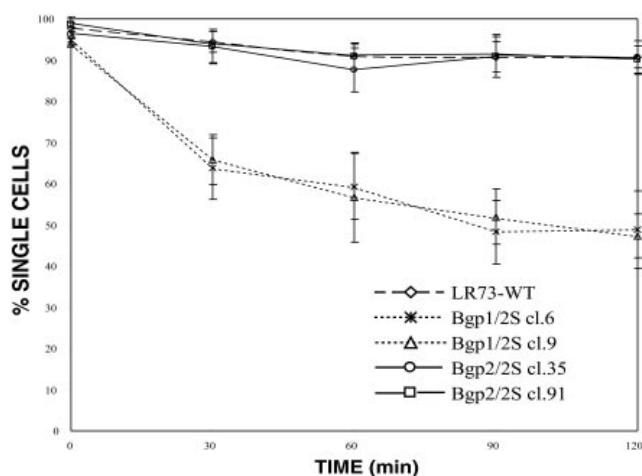


Fig. 7. Aggregation assays. Wild-type and Bgp1/2S-transfected or Bgp2/2S-transfected CHO cell clones were subjected to *in vitro* aggregation assays at 37 °C as described in Materials and methods. Individual cells or aggregates were counted at various time points and plotted as number of single cells vs time. Each assay was repeated in triplicate and standard deviations and errors were computed. (◇) LR73 wild-type; (*) Bgp1/2S clone 6; (Δ) Bgp1/2S clone 9; (○) Bgp2/2S clone 35; (□) Bgp2/2S clone 91.

thereby did not exhibit homophilic adhesion properties (Fig. 7).

DISCUSSION

Although only one *BGP* gene exists in the human and rat, two highly similar *Bgp* genes have been identified on mouse chromosome 7 [3,4]. The *Bgp1* and *Bgp2* genes have conserved very typical exon and intron structures [3,4]. In addition, the first 800 bp of their proximal promoter sequences display 95% identity (P. Nédellec & N. Beauchemin, unpublished observations). These results suggest that the *Bgp1* and *Bgp2* proteins share many characteristics and functions. Surprisingly, the results presented in this report show that the expression patterns and functions of the two proteins are quite distinct.

The first major difference is that the *Bgp1* and *Bgp2* genes do not produce the same type of splice variants. *Bgp1* transcripts encoding two Ig domains are well transcribed in many tissues [23], but the encoded protein seems to be less abundant and is mostly apparent in liver samples [23]. By far the most abundant *Bgp1* proteins in many murine tissues are encoded by *Bgp1* transcripts which include exons 1–5 expressing the four extracellular Ig-like domains. In contrast, in a survey of mouse tissues, the only *Bgp2* transcripts and proteins found are those exhibiting two extracellular Ig domains ([4]; this report). The *Bgp2* gene does include exons 3 and 4 which correspond to the second and third Ig domains (exon 4 exhibits only a one-nucleotide silent mutation relative to the corresponding *Bgp1* exon) and these exons appear to be functional (i.e. no mutations were observed in their splice junctions). However, these exons are apparently used very sparingly, if at all, in expression of *Bgp2* mRNAs and proteins.

Second, the most notable feature of the *BGP* genes lies in the conserved splicing mechanism used to generate isoforms carrying the longer cytoplasmic domain present in every species studied so far. As indicated in Fig. 3, inclusion of the 53-bp exon 7 results in a shift of the ORF and generation of the long tail. A number of important functions have been attributed to this domain. First, the *Bgp1/4L* long tail has potent tumor-suppressor activity [11,31,33]. Secondly, this *Bgp1/4L* isoform is Tyr-phosphorylated by a number of Src-related kinases or the insulin receptor [16,17] and is also Ser-phosphorylated upon activation of protein kinase C [28]. Tyr and Ser phosphorylations are associated with internalization of the insulin receptor [34], neutrophil activation [18], binding of *Bgp1* to the Tyr phosphatases SHP-1 and SHP-2 [16,17], and activation of cellular signal-transduction cascades in response to *N. gonorrea* binding [19]. We have shown here that a *Bgp2* isoform encompassing a 73-amino acid cytoplasmic domain nearly identical with that of the *Bgp1* isoform is expressed in kidney and in a mouse rectal carcinoma cell line. However, this *Bgp2/2L* isoform was not detected by immunoprecipitation from cell lysates. Similarly, the *Bgp2/2L* cDNA could only be obtained using 35 cycles of amplification with nested primers. Very little is known about the regulation of the relative levels of expression of *Bgp1* isoforms *in vivo*: in rat liver, the short and long *Bgp1* isoforms appear to be co-ordinately regulated [35,36]. However, Hunter *et al.* [37] have indicated that, in the NBT II rat bladder carcinoma cells, programmed to exhibit epithelial to mesenchymal transition by treatment with either acidic fibroblast growth factor or other growth factors, the levels of the *Bgp1/4L* isoform were increased 2.5–4.0-fold relative to that of the short tail. The latter remained unchanged in these conditions. These authors

further concluded that the upregulation of the long-tailed isoform was transcriptionally regulated and that the expression of the long and short isoforms could be independently modulated. It remains to be seen whether the expression of the long-tailed *Bgp2* protein will be altered under different physiological conditions.

Similarly, immunocytochemical observations have indicated that *Bgp2* expression is significantly different from that of *Bgp1*. *Bgp2* was not detected in the biliary canaliculi, a characteristic site of the *Bgp1* protein [29]. Although both proteins are found in gut tissue, expression of *Bgp2* is generally found in distinctive cellular sites, i.e. *Bgp2* is restricted to the crypts and is also apparent in some mononuclear cells within the gut. Interestingly, expression of *Bgp2* appeared to be widespread and diffuse in the smooth muscle cytoplasm of blood vessels, gut wall, respiratory and reproductive systems.

The functions of *Bgp2*, other than that of a viral receptor [4], have yet to be defined, but they are clearly different from those of *Bgp1*. *Bgp2* did not function as an adhesion molecule in *in vitro* aggregation assays, whereas the *Bgp1*-expressing transfectant cells formed cellular aggregates readily. This result is consistent with those obtained with the rat *BGP* isoforms exhibiting the same domain topology, i.e. an N-terminal domain and one C2-set Ig-like extracellular domain [38]. Secondly, the expression of *Bgp2* within the crypt region of the small intestine, which represents the most active proliferation area of the gut [39], suggests that this glycoprotein may play an active role in cellular growth, in contrast with *Bgp1/4L* which inhibits tumor cell proliferation [11,12]. Significantly, the long tail of *Bgp1* is the growth-inhibitory domain [31,33] and the mRNA coding for the *Bgp2* isoform expressing this long domain is barely detectable in colon. Finally, *Bgp2* expression was detected in gut mononuclear cells, which suggests a possible role in immune functions. Preliminary evidence gathered from *Bgp2* expression patterns during embryonic development has indicated major expression differences between *Bgp1* and *Bgp2*: whereas *Bgp1* is present consistently in the granulocytic-committed cell lineages [29], *Bgp2* appears exclusively in macrophage-like cells. These hypotheses will be further analysed by functional assays on wild-type hemopoietic progenitor cells, *Bgp1*^{-/-} mutant ES cells and embryos, which are currently being evaluated. Although the *Bgp2* gene appears to be unique in an evolutionary perspective, being found in neither humans nor rats, its expression in the mouse presents us with the possibility of distinguishing between multiple functions potentially mediated by a common *BGP* in humans and rats.

ACKNOWLEDGEMENTS

The authors wish to thank Drs André Veillette, Philippe Gros, Greg Govoni and Cliff Stanners for the gift of cell lines used in this study and numerous experimental suggestions. This work was supported by a grant from the Medical Research Council of Canada to N. B. and by an NIH grant AI26075 to K. V. H. L. I. is a recipient of a Medical Research Council of Canada studentship and N.B. is a senior scholar from the *Fonds de la Recherche en Santé du Québec*.

REFERENCES

1. Stanners, C.P. (1998) In *Cell Adhesion and Communication Mediated by the CEA Family* (Stanners, C.P., ed.), pp. 1–302. Harwood Press, Amsterdam.
2. Robbins, J., Robbins, P.F., Kosak, C.A. & Callahan, R. (1991) The mouse biliary glycoprotein gene (*Bgp*): partial nucleotide

- sequence, expression, and chromosomal assignment. *Genomics* **10**, 583–587.
3. Nédellec, P., Turbide, C. & Beauchemin, N. (1995) Characterization and transcriptional activity of the mouse biliary glycoprotein 1 gene, a carcinoembryonic antigen-related gene. *Eur. J. Biochem.* **231**, 104–114.
 4. Nédellec, P., Dveksler, G.S., Daniels, E., Turbide, C., Chow, B., Basile, A.A., Holmes, K.V. & Beauchemin, N. (1994) Bgp2, a new member of the carcinoembryonic antigen-related gene family, encodes an alternative receptor for mouse hepatitis viruses. *J. Virol.* **68**, 4525–4537.
 5. McCuaig, K., Rosenberg, M., Nédellec, P., Turbide, C. & Beauchemin, N. (1993) Expression of the *Bgp* gene and characterization of mouse colon biliary glycoprotein isoforms. *Gene* **127**, 173–183.
 6. Dveksler, G.S., Dieffenback, C.W., Cardellicchio, C.B., McCuaig, K., Pensiero, M.N., Jiang, G.S., Beauchemin, N. & Holmes, K.V. (1993) Several members of the mouse carcinoembryonic antigen-related glycoprotein family are functional receptors for the coronavirus mouse hepatitis virus-A59. *J. Virol.* **67**, 1–8.
 7. Rojas, M., Fuks, A. & Stanners, C.P. (1990) Biliary glycoprotein, a member of the immunoglobulin supergene family, functions *in vitro* as a Ca²⁺-dependent intercellular adhesion molecule. *Cell Growth Differ.* **1**, 527–533.
 8. Ocklind, C. & Öbrink, B. (1982) Intercellular adhesion of rat hepatocytes. *J. Biol. Chem.* **257**, 6788–6795.
 9. McCuaig, K., Turbide, C. & Beauchemin, N. (1992) mmCGM1a: a mouse carcinoembryonic antigen gene family member, generated by alternative splicing, functions as an adhesion molecule. *Cell Growth Differ.* **3**, 165–174.
 10. Daniels, E., Létourneau, S., Turbide, C., Kuprina, N., Rudinskaya, T., Yazova, A.C., Holmes, K.V., Dveksler, G.S. & Beauchemin, N. (1996) Biliary glycoprotein 1 expression during embryogenesis: correlation with events of epithelial differentiation, mesenchymal-epithelial interactions, absorption, and myogenesis. *Dev. Dynamics* **206**, 272–290.
 11. Kunath, T., Ordoñez-García, C., Turbide, C. & Beauchemin, N. (1995) Inhibition of colonic tumor cell growth by biliary glycoprotein. *Oncogene* **11**, 2375–2382.
 12. Hsieh, J.-T., Luo, W., Song, W., Wang, Y., Van Kleinerman, D.I., N.T. & Lin, S.-H. (1995) Tumor suppressive role of an androgen-regulated epithelial cell adhesion molecule (C-CAM) in prostate carcinoma cell revealed by sense and antisense approaches. *Cancer Res.* **55**, 190–197.
 13. Tanaka, K., Hinoda, Y., Takahashi, H., Sakamoto, H., Nakajima, Y. & Imai, K. (1997) Decreased expression of biliary glycoprotein in hepatocellular carcinomas. *Int. J. Cancer* **74**, 15–19.
 14. Rietdorf, L., Lisboa, B.W., Henkel, U., Naumann, M., Wagener, C. & Loning, T. (1997) Differential expression of CD66a (BGP), a cell adhesion molecule of the carcinoembryonic antigen family, in benign, premalignant and malignant lesions of the human mammary gland. *J. Histochem. Cytochem.* **45**, 957–963.
 15. Bamberger, A.M., Rietdorf, L., Nollau, P., Naumann, M., Erdmann, I., Gotze, J., Brummer, J., Schulte, H.M., Wagener, C. & Loning, T. (1998) Dysregulated expression of CD66a (BGP, C-CAM), an adhesion molecule of the CEA family, in endometrial cancer. *Am. J. Pathol.* **152**, 1401–1406.
 16. Beauchemin, N., Kunath, T., Robitaille, J., Chow, B., Turbide, C., Daniels, E. & Veillette, A. (1997) Association of biliary glycoprotein with protein tyrosine phosphatase SHP-1 in malignant colon epithelial cells. *Oncogene* **14**, 783–790.
 17. Huber, M., Izzi, L., Grondin, P., Houde, C., Kunath, T., Veillette, A. & Beauchemin, N. (1999) The carboxy-terminal region of biliary glycoprotein controls its tyrosine phosphorylation and association with protein tyrosine phosphatases SHP-1 and SHP-2 in epithelial cells. *J. Biol. Chem.* **274**, 335–344.
 18. Skubitz, K.M., Campbell, K.D., Ahmed, K. & Skubitz, A.P.N. (1995) CD66 family members are associated with tyrosine kinase activity in human neutrophils. *J. Immunol.* **151**, 5382–5390.
 19. Hauck, C.R., Meyer, T.F., Lang, F. & Gulbins, E. (1998) CD66 mediate phagocytosis of Opa₅₂ *Neisseria gonorrhoeae* requires a Src-like tyrosine kinase- and Rac1-dependent signalling pathway. *EMBO J.* **17**, 443–454.
 20. Dveksler, G.S., Pensiero, M.N., Cardellicchio, C.B., Williams, R.K., Jiang, G.S., Holmes, K.V. & Dieffenbach, C.W. (1991) Cloning of the mouse hepatitis virus (MHV) receptor: expression in human and hamster cell lines confers susceptibility to MHV. *J. Virol.* **65**, 6881–6891.
 21. Zelus, B.D., Wessner, D.R., Williams, R.K., Pensiero, M.N., Phibbs, F.T., deSouza, M., Dveksler, G.S. & Holmes, K.V. (1998) Purified, soluble recombinant mouse hepatitis virus receptor, Bgp1^b, and Bgp2 murine coronavirus receptors differ in mouse hepatitis virus binding and neutralizing activities. *J. Virol.* **72**, 7237–7244.
 22. Sanger, F., Nicklen, S. & Coulson, A.R. (1977) DNA sequencing with chain-terminating inhibitors. *Proc. Natl Acad. Sci. USA* **74**, 5463–5467.
 23. Rosenberg, M., Nédellec, P., Jothy, S., Fleischer, D., Turbide, C. & Beauchemin, N. (1993) The expression of mouse biliary glycoprotein, a carcinoembryonic antigen-related gene, is down-regulated in malignant mouse tissues. *Cancer Res.* **53**, 4938–4945.
 24. Southern, P.J. & Berg, P. (1982) Transformation of mammalian cells to antibiotic resistance with a bacterial gene under control of the SV40 early region promoter. *J. Mol. Appl. Genet.* **1**, 314–327.
 25. Sambrook, J., Fritsch, E.F. & Maniatis, T. (1989) *Molecular Cloning: A Laboratory Manual*, 2nd edn. Cold Spring Harbor Laboratory Press, Cold Spring Harbor, NY.
 26. Tam, J.P. (1988) Synthetic peptide vaccine design: synthesis and properties of a high-density multiple antigenic peptide system. *Proc. Natl Acad. Sci. USA* **85**, 5409–5413.
 27. Smith, D.B. & Johnson, K.S. (1988) Single-step purification of polypeptides expressed in *Escherichia coli* as fusions with glutathione S-transferase. *Gene* **67**, 31–40.
 28. Edlund, M., Wikstrom, K., Toomik, R., Ek, P. & Öbrink, B. (1998) Characterization of protein kinase C-mediated phosphorylation of the short cytoplasmic domain isoform of C-CAM. *FEBS Lett* **425**, 166–170.
 29. Godfraind, C., Langreth, S.G., Cardellicchio, C.B., Knobler, R., Coutelier, J.P., Dubois-Dalcq, M. & Holmes, K.V. (1995) Tissue and cellular distribution of an adhesion molecule in the carcinoembryonic antigen family that serves as a receptor for the mouse hepatitis virus. *Lab. Invest.* **73**, 615–627.
 30. Watt, S.M., Fawcett, J., Murdoch, S.J., Teixeira, A.M., Gschmeissner, S.E., Hajibagheri, N.M.A.N. & Simmons, D.L. (1994) CD66 identifies the biliary glycoprotein (BGP) adhesion molecule: cloning, expression, and adhesion functions of the BGPc splice variant. *Blood* **84**, 200–210.
 31. Izzi, L., Turbide, C., Houde, C. & Kunath, T., & Beauchemin, N. (1999). *Cis*-determinants in the cytoplasmic domain of CEA-CAM1 responsible for its tumor inhibitory function. *Oncogene* (in press).
 32. Cheung, P.H., Luo, W., Qiu, Y., Zhang, X., Earley, K., Millirons, P. & Lin, S.H. (1993) Structure and function of C-CAM1. The first immunoglobulin domain is required for intercellular adhesion. *J. Biol. Chem.* **268**, 24303–24310.
 33. Turbide, C., Kunath, T., Daniels, E. & Beauchemin, N. (1997) Optimal ratios of biliary glycoprotein isoforms required for inhibition of colonic tumor cell growth. *Cancer Res.* **57**, 2781–2788.
 34. Formisano, P., Najjar, S.M., Gross, C.N., Philippe, N., Oriente, F., Kern-Buell, C.L., Accili, D. & Gorden, P. (1995) Receptor-mediated internalization of insulin. *J. Biol. Chem.* **270**, 24073–24077.
 35. Cheung, P.H., Thompson, N.L., Early, K., Culic, O., Hixson, S. & Lin, S.-L. (1993) Cell-CAM105 isoforms with different adhesion functions are coexpressed in adult rat tissues and during liver development. *J. Biol. Chem.* **268**, 6139–6146.
 36. Thompson, N.L., Panzica, M.A., Hill, G., Lin, S.H., Curran, T.R., Gruppiso, P.A., Baum, O., Reutter, W. & Hixson, D. (1993)

- Spatiotemporal expression of two cell-cell adhesion molecule 105 isoforms during liver development. *Cell Growth Differ.* **4**, 257–268.
37. Hunter, I., Lindh, M. & Öbrink, B. (1994) Differential regulation of C-CAM isoforms in epithelial cells. *J. Cell Sci.* **107**, 1205–1216.
38. Wikstrom, K., Kjellstrom, G. & Öbrink, B. (1996) Homophilic intercellular adhesion mediated by C-CAM is due to a domain 1-domain 1 reciprocal binding. *Exp. Cell Res.* **227**, 360–366.
39. Cheng, H. & Leblond, C.P. (1974) Origin, differentiation and renewal of the four main epithelial cell types in the mouse small intestine. V. Unitarian theory of the origin of the four epithelial cell types. *Am. J. Pathol.* **141**, 537–561.